Published in final edited form as:
Neuroreport. 2012 July 11; 23(10): 590–595. doi:10.1097/WNR.0b013e3283540394.

MicroRNA-320 Induces Neurite Outgrowth by Targeting ARPP-1

Robin E. White and **Rona G. Giffard**
Department of Anesthesia, Stanford University

Abstract

MicroRNAs are important in central nervous system development, functioning, and pathophysiology. Here we demonstrate that increasing levels of microRNA 320 (miR-320) for 3 days markedly increases neurite length and at 4 days reduces total cell number in N2A cells. *In silico* analysis of possible miR-320 targets identified cAMP-regulated phosphoprotein-19 kDa (ARPP-19) and semaphorin 3a (Sema3a) as potential targets that could be involved. ARPP-19 was validated by demonstrating reduced mRNA and protein levels when miR-320 was overexpressed, while miR-320 had no effect on Sema3a expression. ARPP-19 is known to inhibit protein phosphatase-2A (PP2A) activity, which inhibits mitosis and induces neurite outgrowth, making this the likely mechanism. Thus increased levels of miR-320 leads to decreased levels of ARPP-19, increased neurite length, and fewer total cells. These data suggest that miR-320 could play a role in neuronal development and might be a target to enhance neuronal regeneration following injury.

Keywords

microRNA; neurite outgrowth; ARPP-19; PP2A

Introduction

The role of microRNAs in axonal growth during differentiation and injury is a new area of research. Sciatic nerve compression increases expression of miR-188 and miR-500 [1] and decreases expression of miR-320 [2]. Several microRNAs induce neurite outgrowth: miR-21 in dorsal root ganglion cells [3], miR-34a in neural stem cells [4], miR-124 in differentiating P19 cells [5], miR-133b following zebrafish spinal cord injury [6], and both miR-214 [7] and miR-125b [8] in SH-SY5Y cells, while knockdown of miR-541 induces neurite outgrowth in PC12 cells [9]. Although miR-320 is altered in sciatic nerve injury [2], diabetic renal injury [10], and prion disease [11], its role in axonal growth has not been studied. Here we report that overexpression of miR-320 robustly increases neurite length by 3 d and decreases total cell number after 4 d in neuronal Neuro-2A (N2A) cells. Potential targets of miR-320 include Sema3a, an inhibitor of neurite outgrowth [12] and the cAMP-regulated protein ARPP-19, previously shown to inhibit the activity of protein phosphatase (PP2A) [13], an inducer of neurite growth [14]. Although miR-320 overexpression did not attenuate Sema3a expression, miR-320 decreased ARPP-19 mRNA and protein levels. Thus miR-320 decreases ARPP-19 and likely exerts its effects on neurite length and cell number by disinhibiting PP2A activity.

Conflicts of Interest: None declared

Materials and Methods

Cell culture

N2A cells (a kind gift from Drs. Kurt Lucin and Tony Wyss-Coray at Stanford University) passage 5–20 were grown in high-glucose (25 mM) DMEM (Invitrogen, Carlsbad, CA) with 8% fetal bovine serum (Hyclone, Logan, UT) and Penicillin-Streptomycin Solution (50U/ml penicillin, 50 μg/ml Streptomycin; Invitrogen).

miR-320 overexpression

Cells were transfected using FugeneHD (Promega, Madison, WI) with the MXW-PGK-IRES-GFP plasmid (a kind gift from Dr. Chang-Zheng Chen at Stanford University) with or without the pri-miR-320 sequence. DNA containing the pri-miR-320 and ~250 nt flanking sequence on each side were cloned downstream of the PGK promoter in MWX-PGK-IRES-GFP using the forward primer GTAATAGAAGTGGGTGTTGCTG and the reverse primer CGTAGTCTAAGCCACAGTTCTATG. In other experiments, N2A cells were transfected with a control miRNA or miR-320 mimic (10 pM; Applied Biosystems, Carlsbad, CA).

Measurement of neurite outgrowth

One day after plating in 24-well plates (50,000 cells/well), each well was treated with 0.25 μg control or pri-miR-320 plasmid and 1 μl of Fugene HD. Three days after transfection, cells were visualized with a Zeiss AxioVert inverted microscope. Fluorescence images of transfected cells were acquired at 20x magnification using the Zeiss Axiovision software. For each image, the 5 longest neurites were measured using NIH ImageJ and were averaged to give a single value for each well. Using the same images, the percent of transfected cells with neurites and the number of neurites per cell were manually counted.

Evaluation of Cell Number and Cell Death

To assess cell death, cells transfected with pri-miR-320 were stained with propidium iodide (PI; 2.5 μg/ml, dead cells, Sigma, St. Louis, MO) and Hoechst 33342 dye (50 μg/ml, all cells, Sigma #B2261) for 15 min 4 d following transfection, and fluorescence images (20x) were acquired. The number of PI-and Hoechst-stained cells was manually counted and the percentage of dead cells calculated. To assess total cell number cultures were fixed with 4% paraformaldehyde 4 d after transfection and stained with 4′,6-diamidino-2-phenylindole (DAPI; 1:500; Invitrogen). Fluorescence images were acquired at 2.5x magnification and the number of DAPI-stained cells was counted using NIH ImageJ.

Reverse Transcription Quantitative Real-Time Polymerase Chain Reaction (RT-qPCR) for miRNA and mRNA quantitation

Total RNA was isolated with TRIzol® (Invitrogen) 3 d (miRNA) or 4 d (ARPP-19) after transfection. Reverse transcription of miRNA was performed using the TaqMan MicroRNA Reverse Transcription Kit (Applied Biosystems). Equal amounts of RNA (200 ng) were reverse-transcribed with 1.3 mM dNTPs (with dTTP), 50 U reverse transcriptase, 10 U RNase inhibitor, and specific miRNA reverse transcriptase primers (Applied Biosystems) at 16°C for 30 min, 42°C for 30 min, and 85°C for 5 min. PCR reactions were conducted using the TaqManR MicroRNA Assay Kit (0.75 μl of the reaction product and 5 μl 2x Taqman Universal Master Mix in a total volume of 10 μl using the 7900 HT, Applied Biosystems) at 95°C for 10 min, followed by 40 cycles of 95°C for 15 s and 60°C for 1 min. Predesigned primer/probes for miR-320 and mouse U6 (internal control) were also from Applied Biosystems. Measurements were normalized to U6 (ΔCt) and the comparison calculated as the inverse log of ΔΔCt to give a relative fold change value. To measure ARPP-19 mRNA, equal amounts of RNA (600 ng) were reverse-transcribed as above, except random primers

were used at 25°C for 10 min, 37°C for 120 min, and 85°C for 5 min. Quantitation was performed as described above, with ARPP-19 primer and GAPDH as the internal control (Applied Biosystems).

ARPP-19 and Sema3a Immunoblotting

Cells were treated as described above and harvested for protein 4 d following transfection. Immunoblotting was performed as previously described [15]. Briefly, equal amounts (10–20 μg) of protein were loaded and separated on a 4–12% (Sema3a) or 12% (ARPP-19) polyacrylamide gel (Invitrogen), and electrotransferred to Immobilon polyvinylidene fluoride membrane (Millipore Corp., Billerica, MA). Membranes were blocked and incubated overnight with primary antibodies against Sema3a (1:100, sc-28867, Santa Cruz Biotechnologies, Santa Cruz, CA), ARPP-19 (1:1000, G153, a kind gift from Dr. Angus Naim, Yale University [16]), and β-actin (1:5000, A1978, Sigma), then washed and incubated with anti-rabbit and anti-mouse antibodies (1:15000, LiCOR Bioscience, Lincoln, NE). Bands were visualized using the LiCOR Odyssey infrared imaging system. Densitometric analysis of bands was performed using NIH ImageJ and normalized to β-actin.

DotBlot analysis

To measure secreted Sema3a, analysis with the Bio-Dot Microfiltration Apparatus (Biorad, Hercules, CA) was performed. Four hundred μl of media collected 4 d following transfection was loaded into the apparatus and proteins were bound to a nitrocellulose membrane. The membrane was blocked and incubated for 1 h at room temperature with rabbit anti-Sema3a (1:100, Santa Cruz Biotechnologies) then incubated with anti-rabbit antibody (1:15000, LiCOR) for 1 hour at room temperature. Dots were visualized using the LICOR Odyssey infrared imaging system and densitomteric analysis was performed using NIH ImageJ.

Statistical Analysis

Data are expressed as mean +/− standard error of the mean. Student's *t*-tests were used to analyze all data. Differences were considered statistically significant for p-value of < 0.05.

Results

miR-320 increases neurite length and decreases total cell number

To determine if miR-320 increases neurite outgrowth, N2A cells were transfected with a control plasmid or one encoding pri-miR-320, and neurite outgrowth of transfected cells was quantified 3 d later. N2A cells transfected with control plasmid showed primarily stubby neurite outgrowth, while those transfected with pri-miR-320 had greater neurite length, 230% that of control-transfected cells (Figure 1a,b). In contrast, the percentage of cells with neurites did not change between groups (Control = 37.0% +/− 5.8 vs. pri-miR-320 = 44.8% +/− 2.7, $p = 0.25$). The average number of neurites per cell was not significantly different between groups, approximately 2 per cell ($p = 0.13$) (Figure 1c). To determine if pri-miR-320 treatment induced cell death, PI and Hoechst staining was used to assess the cell death in each group. The cell death rate was 6.0% in control transfected cells and 7.3% in cells transfected with pri-miR-320 ($p = 0.69$) (Figure 1d,e). To assess the effect of miR-320 on cell number, cells treated with control or pri-miR-320 plasmid were stained with the nuclear stain DAPI, showing 28% fewer cells with pri-miR-320 treatment (Figure 1f).

ARPP-19 and Sema3a are potential targets for miR-320

Using the TargetScan website, likely targets of miR-320 were identified. Of the potential targets, ARPP-19 had conserved binding sites in the 3′UTRs of 14 species, with 5 potential binding sites in mouse (microrna.org). In addition, ARPP-19 was biologically relevant in that it inhibits the activity of PP2A, which inhibits mitosis and encourages axonal outgrowth [13]. Sema3a, an inhibitor of neurite outgrowth [12], exhibited 1 conserved binding site in the 3′UTRs of 21 mammalian species.

miR-320 decreases ARPP-19 levels

First using RT-qPCR we confirmed that miR-320 levels were altered by transfecting N2A cells with either pri-miR-320 (Figure 2a) or miR-320 mimic (Figure 2b). Pri-miR-320 increases miR-320 50-fold while miR-320 mimic increased miR-320 levels 250-fold. Since miRNA can lead to reduced protein levels either by translational arrest or degradation of mRNA, we assessed levels of ARPP-19 mRNA following transfection. Both pri-miR-320 (Figure 2c) and miR-320 mimic (Figure 2d) reduced ARPP-19 mRNA levels 20% and 48%, respectively, consistent with message degradation. We then determined the level of ARPP-19 protein in cells transfected with miR-320 mimic, as this had the greater effect on miR-320 levels. Treatment of N2A cells with miR-320 mimic decreased ARPP-19 levels by 63% compared to control (Figure 3a,b), suggesting that miR-320 may affect neurite length and cell number via ARPP-19 and PP2A (Figure 3c).

miR-320 does not decrease Sema3a levels

To determine if inhibition of Sema3a is an additional mechanism of miR-320-induced neurite growth, cellular and secreted Sema3a were measured. Little cellular Sema3a was detected in N2A cells, and levels did not significantly change with transfection with either pri-miR-320 (Figure 4a,b) or miR-320 mimic (Figure c,d). Likewise, transfection of N2A cells with miR-320 mimic had no effect on secreted Sema3a (Figure 4e,f).

Discussion

In this study we show that miR-320 increases neurite length and leads to lower numbers of N2A cells, a likely result of decreased ARPP-19 and subsequent disinhibition of PP2A activity. As no increase in cell death was observed with miR-320 overexpression, the lower cell number was likely due to decreased cell division, an effect of PP2A activity. Thus far 3 targets have been verified for miR-320: the PTEN component ETS2 [17], histone deacetylase 4 [18], and the transferrin receptor CD71 [19]. None of these targets have been implicated in neurite outgrowth, but ETS2 is required for breast cell proliferation [20] and CD71 enhances proliferation in B-cell lymphoma cells [21]. These studies suggest that miR-320's actions on either ETS2 or CD71 may contribute to the observed lower cell number, but the importance of ETS2 and CD71 has not yet been explored in N2A cells.

Recent studies have identified a key interaction between ARPP-19 and PP2A, with downstream effects on cell proliferation and neurite growth. ARPP-19 is a cAMP-regulated phosphoprotein that is a substrate for protein kinase C [13] and is expressed ubiquitously in the cortex and striatum of the mammalian brain [16]. PP2A is a phosphatase responsible for dephosphorylating mitotic proteins such as cdc2 [22]. Recently, Gharbi-Ayachi et al. [13] demonstrated that ARPP-19 binds to PP2A and inhibits its activity [13]. Furthermore, a study using N2A cells and primary hippocampal neurons showed that overexpression of PP2A increased neurite length [14]. Thus our observations of increased neurite length and reduced cell number with miR-320 overexpression are consistent with reduced ARPP-19, allowing greater PP2A activity.

Although *in silico* analysis reveals Sema3a as a potential target of miR-320, overexpression of miR-320 in N2A cells did not affect Sema3a protein expression. This may be due to a number of factors, including the modest baseline level of Sema3a in N2A cells, and cell-specific differences in miRNA effects, shown in other model systems [23].

Neurodegenerative diseases and acute injuries are characterized by dysfunction in axonal outgrowth or lack of regeneration of axons, for example amyotropic lateral sclerosis [24] and spinal cord injury [25]. The current lack of clinical treatments that encourage axon growth may reflect the possibility that manipulation of a single gene or protein may not be sufficient for successful treatment. As microRNAs potentially regulate several related targets, they are promising candidates for therapeutics. Indeed, clinical trials of miRNA-based drugs have already begun. Here we have shown that miR-320 dramatically increases neurite length. Future studies should examine the potential of miR-320 to enhance axonal growth *in vivo* and look for additional targets that may also contribute to this effect.

Acknowledgments

This work was supported in part by NIH grants R01 GM49831 to RGG and T32 GM089626 to REW. The authors thank Yu Lu for construction of the pri-miR-320 vector and all members of the Giffard Laboratory for helpful discussions, especially Yi-Bing Ouyang, Xiaoyun Sun, and Ludmila Volobouéva.

References

1. Zhou S, Yu B, Qian T, Yao D, Wang Y, Ding F, et al. Early changes of microRNAs expression in the dorsal root ganglia following rat sciatic nerve transection. Neurosci Lett. 2011; 494:89–93. [PubMed: 21371527]
2. Rau CS, Jeng JC, Jeng SF, Lu TH, Chen YC, Liliang PC, et al. Entrapment neuropathy results in different microRNA expression patterns from denervation injury in rats. BMC Musculoskelet Disord. 2010; 11:181. [PubMed: 20704709]
3. Strickland IT, Richards L, Holmes FE, Wynick D, Uney JB, Wong LF. Axotomy-induced miR-21 promotes axon growth in adult dorsal root ganglion neurons. PLoS One. 2011; 6:e23423. [PubMed: 21853131]
4. Aranha MM, Santos DM, Sola S, Steer CJ, Rodrigues CM. miR-34a regulates mouse neural stem cell differentiation. PLoS One. 2011; 6:e21396. [PubMed: 21857907]
5. Yu JY, Chung KH, Deo M, Thompson RC, Turner DL. MicroRNA miR-124 regulates neurite outgrowth during neuronal differentiation. Exp Cell Res. 2008; 314:2618–33. [PubMed: 18619591]
6. Yu YM, Gibbs KM, Davila J, Campbell N, Sung S, Todorova TI, et al. MicroRNA miR-133b is essential for functional recovery after spinal cord injury in adult zebrafish. Eur J Neurosci. 2011; 33:1587–97. [PubMed: 21447094]
7. Chen H, Shalom-Feuerstein R, Riley J, Zhang SD, Tucci P, Agostini M, et al. miR-7 and miR-214 are specifically expressed during neuroblastoma differentiation, cortical development and embryonic stem cells differentiation, and control neurite outgrowth in vitro. Biochem Biophys Res Commun. 2010; 394:921–7. [PubMed: 20230785]
8. Le MT, Xie H, Zhou B, Chia PH, Rizk P, Um M, et al. MicroRNA-125b promotes neuronal differentiation in human cells by repressing multiple targets. Mol Cell Biol. 2009; 29:5290–305. [PubMed: 19635812]
9. Zhang J, Liu LH, Zhou Y, Li YP, Shao ZH, Wu YJ, et al. Effects of miR-541 on neurite outgrowth during neuronal differentiation. Cell Biochem Funct. 2011; 29:279–86. [PubMed: 21452340]
10. Chen YQ, Wang XX, Yao XM, Zhang DL, Yang XF, Tian SF, et al. Abated microRNA-195 expression protected mesangial cells from apoptosis in early diabetic renal injury in mice. J Nephrol. 2011:0. [PubMed: 21983986]
11. Saba R, Goodman CD, Huzarewich RL, Robertson C, Booth SA. A miRNA signature of prion induced neurodegeneration. PLoS One. 2008; 3:e3652. [PubMed: 18987751]

12. He Z, Tessier-Lavigne M. Neuropilin is a receptor for the axonal chemorepellent Semaphorin III. Cell. 1997; 90:739–51. [PubMed: 9288753]
13. Gharbi-Ayachi A, Labbe JC, Burgess A, Vigneron S, Strub JM, Brioudes E, et al. The substrate of Greatwall kinase, Arpp19, controls mitosis by inhibiting protein phosphatase 2A. Science. 2010; 330:1673–7. [PubMed: 21164014]
14. Liu D, Zheng HY, Luo ZZ, Wang Q, Zhu LQ. Effect of PP-2A on neurite outgrowth in neuronal cells. In Vitro Cell Dev Biol Anim. 2010; 46:702–7. [PubMed: 20585893]
15. Han RQ, Ouyang YB, Xu L, Agrawal R, Patterson AJ, Giffard RG. Postischemic brain injury is attenuated in mice lacking the beta2-adrenergic receptor. Anesth Analg. 2009; 108:280–7. [PubMed: 19095863]
16. Girault JA, Horiuchi A, Gustafson EL, Rosen NL, Greengard P. Differential expression of ARPP-16 and ARPP-19, two highly related cAMP-regulated phosphoproteins, one of which is specifically associated with dopamine-innervated brain regions. J Neurosci. 1990; 10:1124–33. [PubMed: 2158525]
17. Bronisz A, Godlewski J, Wallace JA, Merchant AS, Nowicki MO, Mathsyaraja H, et al. Reprogramming of the tumour microenvironment by stromal PTEN-regulated miR-320. Nat Cell Biol. 2011
18. Fukushima T, Taki K, Ise R, Horii I, Yoshida T. MicroRNAs expression in the ethylene glycol monomethyl ether-induced testicular lesion. J Toxicol Sci. 2011; 36:601–11. [PubMed: 22008535]
19. Schaar DG, Medina DJ, Moore DF, Strair RK, Ting Y. miR-320 targets transferrin receptor 1 (CD71) and inhibits cell proliferation. Exp Hematol. 2009; 37:245–55. [PubMed: 19135902]
20. Xu D, Dwyer J, Li H, Duan W, Liu JP. Ets2 maintains hTERT gene expression and breast cancer cell proliferation by interacting with c-Myc. J Biol Chem. 2008; 283:23567–80. [PubMed: 18586674]
21. O'Donnell KA, Yu D, Zeller KI, Kim JW, Racke F, Thomas-Tikhonenko A, et al. Activation of transferrin receptor 1 by c-Myc enhances cellular proliferation and tumorigenesis. Mol Cell Biol. 2006; 26:2373–86. [PubMed: 16508012]
22. Lee TH, Turck C, Kirschner MW. Inhibition of cdc2 activation by INH/PP2A. Mol Biol Cell. 1994; 5:323–38. [PubMed: 8049524]
23. Liu X, Cheng Y, Yang J, Xu L, Zhang C. Cell-specific effects of miR-221/222 in vessels: Molecular mechanism and therapeutic application. J Mol Cell Cardiol. 2012; 52:245–55. [PubMed: 22138289]
24. Gordon T, Hegedus J, Tam SL. Adaptive and maladaptive motor axonal sprouting in aging and motoneuron disease. Neurol Res. 2004; 26:174–85. [PubMed: 15072637]
25. Fitch MT, Silver J. CNS injury, glial scars, and inflammation: Inhibitory extracellular matrices and regeneration failure. Exp Neurol. 2008; 209:294–301. [PubMed: 17617407]

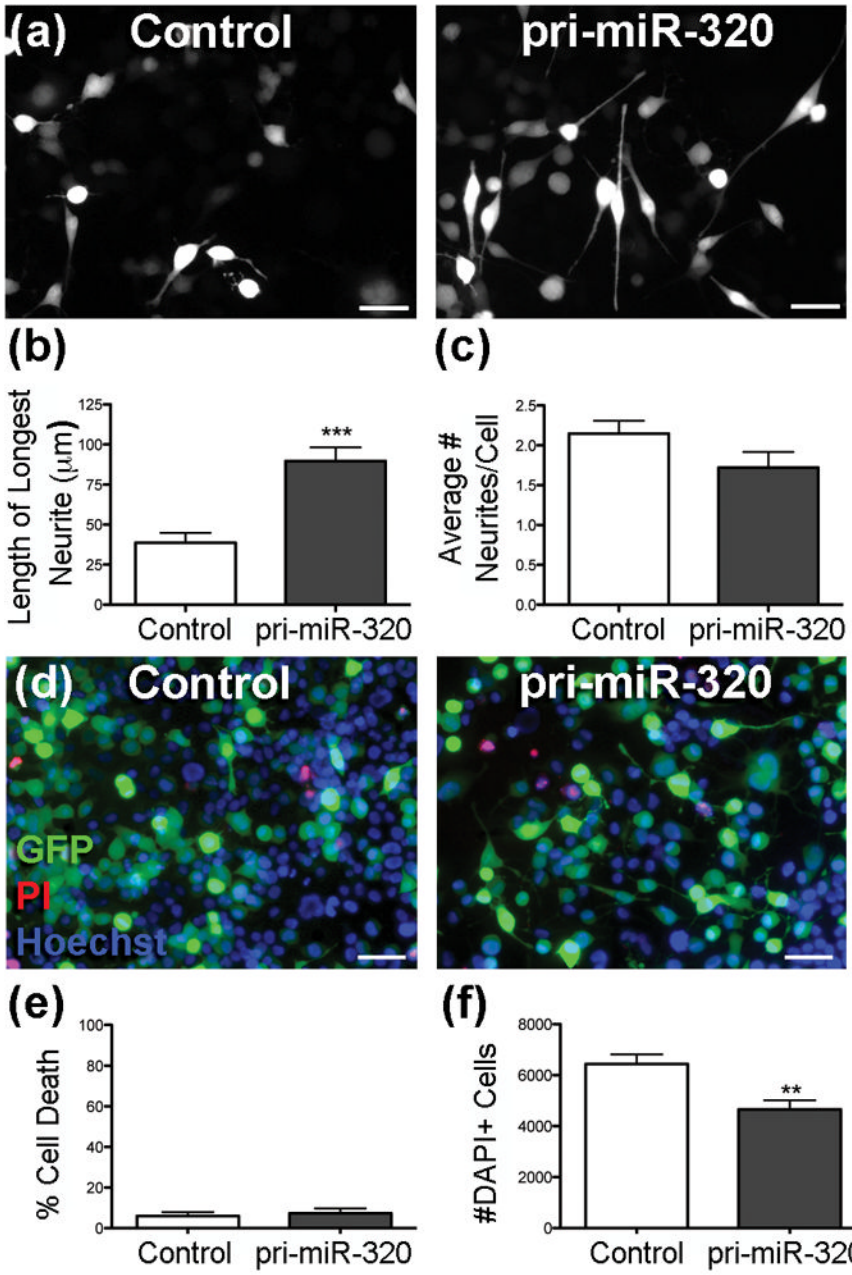

Figure 1.

pri-miR-320 increases maximum neurite length and limits cell number. (a) Fluorescence micrographs showing representative images of N2A cells transfected with a control plasmid (control) or plasmid containing pri-miR-320. Scale = 50 μm. (b–c) Quantification of maximum neurite length (b) and the average number of neurites per cell (c) in transfected cells (n = 5–6 cultures/group, p = 0.13). (d) Representative images of cells transfected with a control plasmid (control) or a plasmid containing pri-miR-320 and stained with PI (red) and Hoechst (blue). The green cells express GFP from the transfection plasmid. Note that few cells stain with PI. Scale = 50 μm. (e) Quantification of cell death following transfection (n = 4 cultures/group). (f) Quantification of DAPI+ cells after transfection with control or pri-miR-320 plasmid (n = 4 cultures/group). **p < 0.01, ***p < 0.001 compared to control.

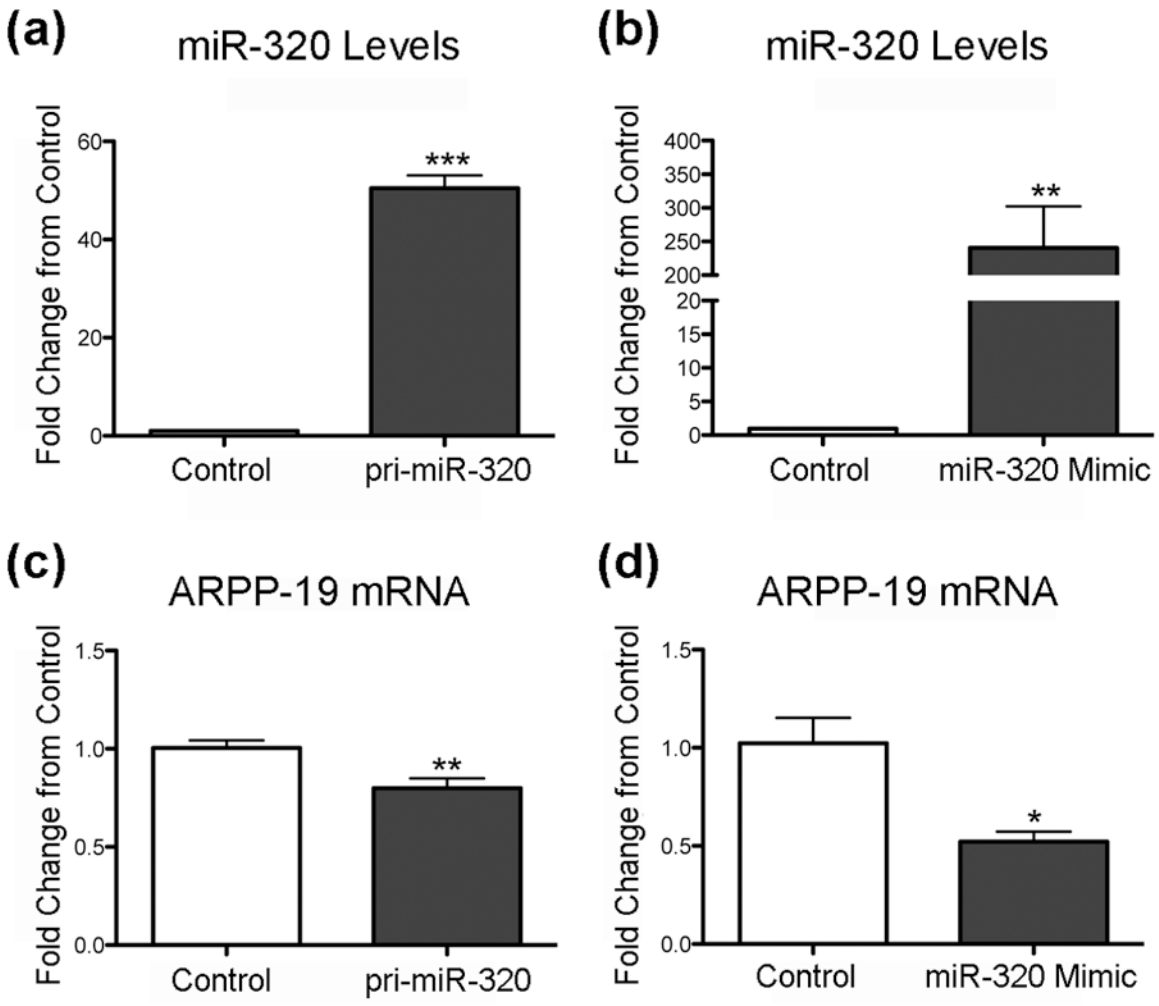

Figure 2.

Increasing miR-320 decreases ARPP-19 mRNA levels. (a,b) RT-qPCR analysis of miR-320 levels after transfection with (a) pri-miR-320 (n = 6 cultures/group) or (b) miR-320 Mimic (n = 4 cultures/group). RT-qPCR analysis of ARPP-19 mRNA levels after transfection with (c) pri-miR-320 (n = 6 cultures/group) or (d) miR-320 Mimic (n = 4 cultures/group). *$p < 0.05$, **$p < 0.01$, ***$p < 0.001$ compared to control. Mimic induced much higher levels of miR-320 and lower levels of mRNA for ARPP-19.

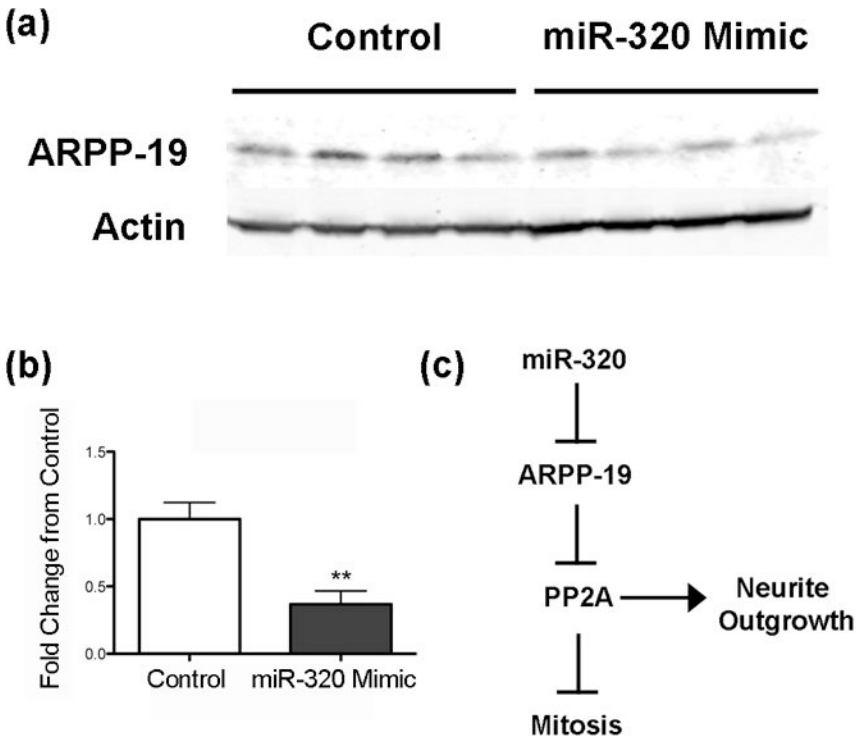

Figure 3.

Increasing miR-320 levels decreases ARPP-19 protein levels. (a) Immunoblot of cells transfected with control or pri-miR-320 plasmid, then probed with an antibody to ARPP-19. (b) Quantification showing that transfection with miR-320 mimic decreases ARPP-19 expression 63%. **$p < 0.01$ compared to control after normalizatian to actin as the loading control, $n = 4$ cultures/group. (c) Schematic showing potential signaling pathway by which miR-320-induces neurite growth via inhibition of ARPP-19 and activation of PP2A.

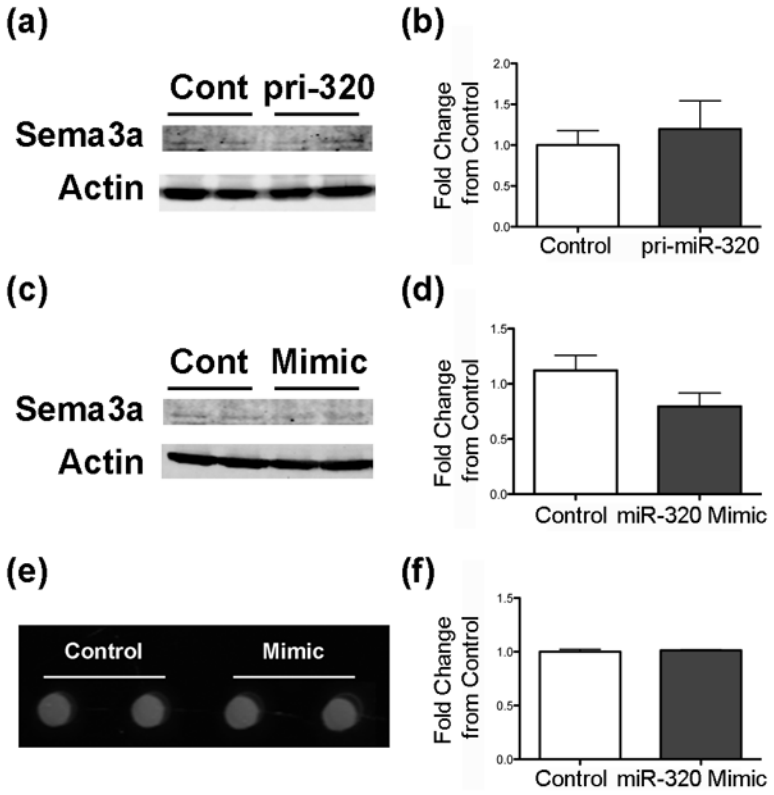

Figure 4.

miR-320 does not decrease Sema3a in N2A cells. Immunoblots of N2A cells treated with either (a,b) pri-miR-320 (n = 6 cultures/group, p = 0.62) or (c,d) miR-320 mimic (n = 4 cultures/group, p = 0.12) and probed with an antibody against Sema3a. (e-f) Representative image of a DotBlot (e) and quantification (f) of the levels of Sema3a in medium of cells transfected with control or miR-320 mimic (n = 3 cultures/group, p = 0.64).